Noname manuscript No.
(will be inserted by the editor)

Kinematic oscillations of railway wheelsets

Mate Antali · Gabor Stepan · S. John Hogan

Last version: 2015.12.16.

Abstract We show that Klingel's classical formula for the frequency of the small kinematic oscillations of railway wheelsets results in a significant error even in the simplest physically relevant cases. The exact 3D nonlinear equations are derived for single contact point models of conical wheels and cylindrical rails. We prove that the resulting nonlinear system exhibits periodic motions around steady rolling, which consequently is neutrally stable. The linearised equations provide the proper extension of Klingel's formula. Our results serve as an essential basis for checking multibody dynamics models and codes used in railway dynamics.

Keywords railway wheelset, nonholonomic system, kinematic oscillation, Klingel's formula

1 Introduction

The conical profile of railway wheelsets is one of the oldest and most important inventions in railway engineering. It provides effective guidance of the vehicle on a curved track by varying rolling radii of the wheels (see Figure 1).

Mate Antali
Department of Applied Mechanics, Budapest University of Technology and Economics, Budapest, H-1521, Hungary
E-mail: antali@mm.bme.hu

Gabor Stepan
Department of Applied Mechanics, Budapest University of Technology and Economics, Budapest, H-1521, Hungary
E-mail: stepan@mm.bme.hu

John Hogan
Department of Engineering Mathematics, University of Bristol, Queen's Building, University Walk, Bristol BS8 1TR, UK
E-mail: s.j.hogan@bristol.ac.uk

Gabor Stepan
HAS-BME Research Group on Dynamics of Machines and Vehicles, Hungarian Academy of Sciences, Budapest H-1521, Hungary

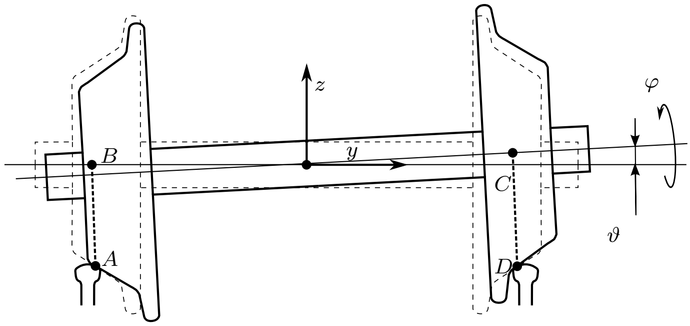

Fig. 1 Change of the rolling radii on a curved track. The lateral and vertical displacements of the geometric centre are denoted by y and z, respectively. The pitch angle is denoted by ϑ, and the roll angle φ corresponds to the rotation of the wheelset around its principal axis of rotation.

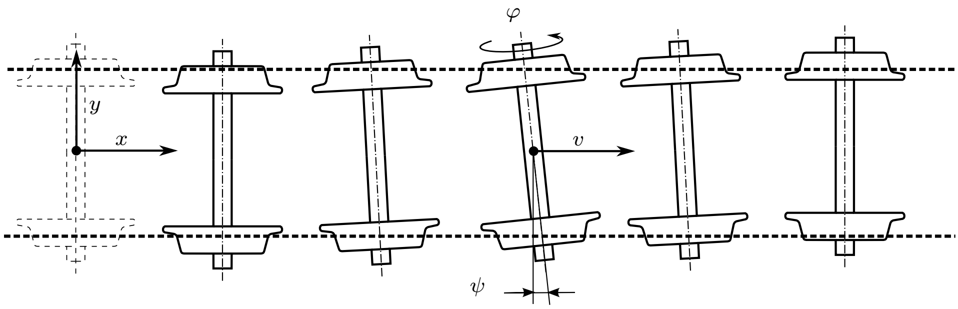

Fig. 2 Kinematic oscillation on a straight track. The longitudinal and lateral displacements of the geometric centre are denoted by x and y, respectively. The yaw angle is denoted by ψ, its projection on the horizontal plane is shown in the figure, and the roll angle φ corresponds to the rotation of the wheelset around its principal axis of rotation.

v	velocity of the vehicle (see Fig. 2)
α	half-angle of the approximating cone
h	conicity of the wheelset (tangent of α)
d_0,R_0	nominal semi-gauge and nominal rolling radius
d	semi-distance of the approximating cylinders of the rails
R	radius of the base circle of the approximating cone of the wheelset
r	radius of the approximating cylinders of the rails
k,l	dimensionless parameters related to R and r, respectively (see Eqn. (27))
ω	angular frequency of the kinematic oscillation (see Eqn. (56))
ω_K	approximate angular frequency according to Klingel's formula (see Eqn. (7))

Table 1 List of geometric and kinematic parameters (see Figures 2 and 3)

x, y, z	longitudinal, lateral and vertical translation of the centre of the wheelset
φ	roll angle of the rotation of the wheelset around its axis of rotational symmetry
ψ, ϑ	yaw and pitch angles of the axis of rotational symmetry
$\chi^{\pm}, \delta^{\pm}$	surface parameters of the contact point on the left ($^{+}$) or right ($^{-}$) wheel
$\xi^{\pm}, \gamma^{\pm}$	surface parameters of the contact point on the left ($^{+}$) or right ($^{-}$) rail

Table 2 List of state variables (see Figures 1, 2 and 4)

However, conicity of the wheelset has a serious side-effect which is usually called kinematic oscillation [24]. This vibration is superposed on the steady rolling of the wheelset, and represents a 3D motion which is usually described by lateral displacement and yaw (see Figure 2). This was observed by George Stephenson [8], and the first analytical study was carried out by Klingel [12]. Several extensions of Klingel's theory appeared later partly related to the non-conical wheel profiles, partly related to wear [[6],[24],[10]]. Klingel's theory is linear both in terms of the state variables and some of the parameters. Attempts to provide geometric nonlinear extensions can be found in the works of de Pater ([19], [20] and [5]).

As stated by Iwnicki [8], this kinematic oscillation is modified by the effects of creep. When combined with creep, the resulting oscillation is called hunting. Carter [3] derived the equations including creep, from which the critical speed can be determined above which steady rolling is unstable to hunting. Carter's model has been further extended with improved creep and stick-slip models, summarized in the books of Johnson [9] and Kalker [11]. More recent models include material nonlinearities and the effects of the flanges ([14], [16], [1], [23], [22] and [7]). For a detailed historic overview see [13] and [26].

In the current paper we deal with the kinematic oscillations in the absence of creep. We obtain analytical results which can serve as an important tool for checking both multibody software and specific railway dynamics software. For small amplitude oscillations, this means that Klingel's formula needs to be modified when the product of the sine of the half-angle α and the ratio of the radius r and the semi-gauge d is not negligible (see Figure 3). For large amplitudes, we prove that the kinematic oscillations are periodic leading to a neutrally stable steady rolling. These two results provide an effective numerical challenge for current multibody software.

The paper is organised as follows. In Section 2, we give an overview on existing kinematic oscillation models of railway wheelsets focusing on Klingel's theory and its current linear and nonlinear extensions. In Section 3, we construct the fully nonlinear single contact point model in 3D assuming arbitrary conical wheelsets and cylindrical rails. In Section 4, we derive the exact governing equations of the system, and obtain the simplest possible second order nonlinear differential equation, which fully determines the 3D motion. In Section 5, we linearise the system to obtain a proper extension of Klingel's formula, and we also show that the fully nonlinear system has a conserved quantity, a pseudo-energy function.

2 Overview of kinematic oscillation models

2.1 Klingel's formula

Klingel's famous model for the small oscillations of a single wheelset was published in 1883 [12]. It can be derived using Rendtenbacher's geometric relation ([26], p. 5). An essentially similar derivation can be performed using the rolling constraint directly, as follows.

A single wheelset is considered with a conical profile rolling on two parallel cylindrical rails, which is the simplest physically relevant arrangement for modelling kinematic oscillations. The half cone angle of the wheelset is denoted by α, and the radius of the cylindrical rails is r (see Figure 3, left panel, and Tables 1 and 2 for the list of the parameters and the state variables). During stationary rolling of the wheelset, the distance of the contact points is $2d_0$, and the rolling radius is denoted by R_0.

The derivation of Klingel's formula is called *linearised*, not only in the sense that the pitch angle ϑ and the yaw angle ψ are considered to be small, but also including the assumptions $\alpha \ll 1$ and $r \ll d_0$. In other words, linearisation is carried out not only in the variables but also in some of the parameters. When the symbol $\approx$ is used in this section, it includes all these approximations.

The model is usually derived for the lateral displacement y and the yaw angle ψ. From Figure 2 it can be seen that

$$\dot{y} \approx v\psi., \tag{1}$$

where v denotes the constant velocity of the geometric centre of the wheelset along the track.

If ideal rolling is assumed, then the two contact points of the wheelset have zero velocity. Therefore the direction of the angular velocity vector $\boldsymbol{\omega}$ must be parallel to the vector $\mathbf{r}_{AD}$ in Figure 1, which leads to

$$\boldsymbol{\omega} \times \mathbf{r}_{AD} = \mathbf{0}, \tag{2}$$

where $\times$ means the vector product. The vectors between the contact points A and D and their projections to the symmetry axis of the wheelset, C and D, can be approximated by

$$\mathbf{r}_{AB} \approx \begin{bmatrix} 0 \\ 0 \\ R_0 - hy \end{bmatrix}, \qquad \mathbf{r}_{BC} \approx \begin{bmatrix} 0 \\ 2d_0 \\ 0 \end{bmatrix}, \qquad \mathbf{r}_{CD} \approx \begin{bmatrix} 0 \\ 0 \\ -R_0 - hy \end{bmatrix}, \tag{3}$$

where $h := \tan\alpha$ is the conicity of the wheelset. From these, the vector $\mathbf{r}_{AD} = \mathbf{r}_{AB} + \mathbf{r}_{BC} + \mathbf{r}_{CD}$ can be determined. The angular velocity can be approximated as

$$\boldsymbol{\omega} \approx \begin{bmatrix} 0 \\ v/R_0 \\ \dot{\psi} \end{bmatrix}. \tag{4}$$

By substituting these into (2) we get

$$\dot{\psi} \approx -\frac{hv}{R_0 d_0} y. \tag{5}$$

From (1) and (5) we can see that

$$\ddot{y} \approx -\omega_K^2 y \tag{6}$$

where ω_K is an approximation to the angular frequency ω of small oscillations of the wheelset given by

$$\omega \approx \omega_K := v\sqrt{\frac{h}{R_0 d_0}}, \tag{7}$$

which is called Klingel's formula. It is usually not mentioned in the literature, that the approximate angular frequency ω_K includes the parametric linearisation assumptions $\alpha \ll 1$ and $r \ll d_0$. In the current paper we will show, that without these assumptions this derivation cannot be done. Ignoring these assumptions requires a complete nonlinear derivation, which results an improved formula for the accurate value ω.

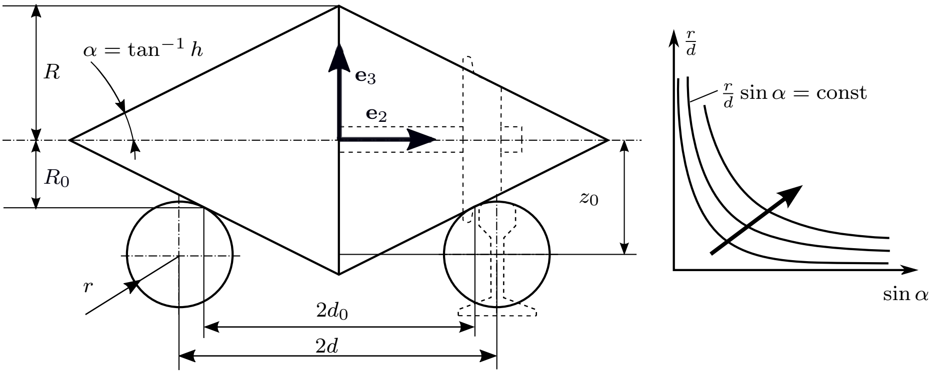

Fig. 3 Left panel: Modelling the geometry of wheelset and rails. The parameter set (α, d_0, R_0, r) can be chosen independently, the other parameters are given by: $h := \tan\alpha$, $z_0 := R_0 + r\cos\alpha$, $R := R_0 - d_0\tan\alpha$ and $d := d_0 + r\sin\alpha$. Right panel: Relative error of Klingel's formula depending on parameters. Each curve corresponds to a constant relative error, computed from (57). The arrow shows the direction of increasing error of the formula.

2.2 Corrections of Klingel's model and general approach

Recent corrections of Klingel's formula are mainly based on the notion of *equivalent conicity*, denoted by h^*, which is defined using an empirically known value of ω, by

$$h^* := \frac{v^2 R_0 d_0}{\omega^2}. \tag{8}$$

The motivation is to have an accurate frequency value when h is replaced by h^* in (7). Several approximations of the equivalent conicity have been developed (see e.g. [6], [10], or [2] for an overview). Let us now consider Joly's correction [10] for concave wheel profiles:

$$h^*_J = \frac{r_w}{r_w - r} h, \tag{9}$$

where r_w is the curvature radius of the profile at the contact point. If we check the case when the wheel is purely conical, that is, $r_w \to \infty$, we obtain $h^*_J \to h$, which is the conicity itself. Thus, on one hand, (9) includes an arbitrary value of r, on the other hand, it reproduces Klingel's approximation for conical wheelsets, which is valid only for $r \ll R_0$.

This and other improvements are based on the assumption that Klingel's formula is correct for conical wheelsets and cylindrical rails. But we will see that it is not accurate when finite values of r and α are assumed. A nonlinear derivation is essential to create the correction of Klingel's formula even for the simplest geometries.

De Pater clearly realised the importance of nonlinear effects for full 3D motion, and performed calculations in [19], [20] and [5]. In these models arbitrary profiles of the wheelset and the rails are allowed, and the description is extended not only to the kinematic oscillation, but to the full hunting motion with creep effects. However his models proved to be too general, as he succeeded in obtaining only numerical results, and no analytical corrections.

In the current paper the kinematic oscillations of the conical wheelset is investigated through a full nonlinear extension, and the correct differential equations are derived instead of (1) and (5). From these the accurate expression of the angular frequency of the small kinematic oscillations can be obtained, which is a correction of Klingel's formula.

3 Mechanical model

We investigate the problem of a single wheelset travelling along a straight track. Both the wheelset and the rails are modelled as rigid bodies, and single contact points are assumed between the wheelset and each of the rails. The use of rigid body models is an accepted and justified assumption for the global dynamics, since wheel-rail deformations are concentrated in a tiny region of the contact area only. In the meantime, the assumption of single contact points has two significant effects on the model. On the one hand, it reduces the dimension of the dynamics of the system, on the other hand, it neglects the possible stabilizing or destabilizing effect of the local deformations, i. e. the creep forces. Consequently, our applied assumptions make it possible to investigate the kinematic oscillation separately. Clearly, the single contact point model is a limiting case of creep force models, as the load of the wheels decreases and/or the local stiffness of the wheel increases.

We proceed as follows. The unconstrained wheelset has 6 degrees of freedom (DoF). Two DoF are constrained by the geometric constraints between the surfaces of the wheelset and each of the rails. Pure rolling can be expressed by kinematic constraints, which means two nonholonomic scalar equations for each contact point. We will show that this set of nonholonomic constraints is redundant, and results in 3 independent scalar equations. Therefore the number of the degrees of freedom of the purely rolling wheelset is given by 6-2-3=1. If the movement of the wheelset is prescribed along the track, then this last DoF is also constrained. Therefore the 3D motion of the wheelset is fully determined by kinematics alone, without the need for Newton's equations. That is why it was named kinematic oscillation.

3.1 Motion of the wheelset

The motion of the rigid wheelset is described by a displacement $\mathbf{u} : \mathbb{R}^3 \to \mathbb{R}^3$, which is made up of a rotation and a translation:

$$\mathbf{u}(\mathbf{r}) := \mathbf{R}\,\mathbf{r} + \mathbf{x}. \tag{10}$$

Here $\mathbf{r}$ denotes a point of the wheelset in a given reference state, and $\mathbf{u}(\mathbf{r})$ is the position of the point in the current state. The translation vector $\mathbf{x} \in \mathbb{R}^3$ is parametrised by Cartesian coordinates, $\mathbf{x} := \begin{bmatrix} x \; y \; z \end{bmatrix}^{\mathrm{T}}$. The rotation tensor $\mathbf{R} \in \mathbb{R}^{3\times 3}$ is an orthonormal matrix parametrised by Euler angles $(\vartheta, \psi, \varphi)$ called pitch, yaw and roll angles, respectively, and given by

$$\mathbf{R} := \begin{bmatrix} 1 & 0 & 0 \\ 0 & \cos\vartheta & -\sin\vartheta \\ 0 & \sin\vartheta & \cos\vartheta \end{bmatrix} \cdot \begin{bmatrix} \cos\psi & -\sin\psi & 0 \\ \sin\psi & \cos\psi & 0 \\ 0 & 0 & 1 \end{bmatrix} \cdot \begin{bmatrix} \cos\varphi & 0 & \sin\varphi \\ 0 & 1 & 0 \\ -\sin\varphi & 0 & \cos\varphi \end{bmatrix}, \tag{11}$$

where $\vartheta \in [-\pi, \pi)$, $\psi \in (-\pi/2, \pi/2)$ and $\varphi \in [0, 2\pi)$. The meanings of ψ, ϑ and φ are shown in Figures 1 and 2.

Hence, the current position of the wheelset can be described by six scalar variables: x and φ are related to the steady rolling of the wheelset without oscillation, and y,z,ϑ,ψ describe kinematic oscillation.

If $\mathbf{x}$ and $\mathbf{R}$ are functions of time, then the derivative of $\mathbf{u}$ gives the Lagrangian velocity field

$$\mathbf{v}(\mathbf{r}) := \dot{\mathbf{u}}(\mathbf{r}) = \mathbf{R}\boldsymbol{\Omega}\mathbf{r} + \dot{\mathbf{x}}, \tag{12}$$

where the dot denotes differentiation with respect to time, and $\boldsymbol{\Omega} := \mathbf{R}^{-1}\dot{\mathbf{R}}$ is the angular velocity in tensor form. For a full explanation of the meaning and importance of $\boldsymbol{\Omega}$ see [17], p.26. We find that $\dot{\mathbf{x}} = \begin{bmatrix} \dot{x} \ \dot{y} \ \dot{z} \end{bmatrix}^{\mathrm{T}}$, and

$$\boldsymbol{\Omega} = \begin{bmatrix} 0 & -\dot{\vartheta}\cos\psi\sin\varphi - \dot{\psi}\cos\varphi & \dot{\varphi} - \dot{\vartheta}\sin\psi \\ \dot{\vartheta}\cos\psi\sin\varphi + \dot{\psi}\cos\varphi & 0 & -\dot{\vartheta}\cos\psi\cos\varphi + \dot{\psi}\sin\varphi \\ -\dot{\varphi} + \dot{\vartheta}\sin\psi & \dot{\vartheta}\cos\psi\cos\varphi - \dot{\psi}\sin\varphi & 0 \end{bmatrix}. \tag{13}$$

3.2 Geometry of the track

Rail profiles are usually constructed from arcs and straight lines. During normal contact of the wheelset and the rails, the contact point is on the upper arc of the profile having a radius r. That is the reason for modelling the straight track as two infinite parallel cylinders, whose symmetry axes are at a distance of $2d$ apart (see Figure 3).

The left and right rails are described by parametric surfaces denoted by $\boldsymbol{\rho}^+$ and $\boldsymbol{\rho}^-$, respectively. The definition of $\boldsymbol{\rho}^\pm$ in a frame with an orthonormal coordinate system $(\mathbf{e}_1, \mathbf{e}_2, \mathbf{e}_3)$ fixed to the track is:

$$\boldsymbol{\rho}^\pm(\xi,\gamma) := \begin{bmatrix} \xi \\ r\sin\gamma \pm d \\ r\cos\gamma - z_0 \end{bmatrix}, \tag{14}$$

where $\xi \in (-\infty, \infty)$ and $\gamma \in [-\pi, \pi)$ are the rail surface parameters. The surface parametrisation and coordinate directions are sketched in Figure 4.

3.3 Geometry of the wheelset

A common property of most wheel profiles is a tilted line segment around the usual location of the contact point. Other parts of the profile are excluded from our analysis as well as the change of the profile due to wear (see [28]). Thus the whole wheelset can be considered as a bicone, that is two identical circular straight cones glued together at their bases, as shown in Figure 3. The half cone angle is denoted by α, and R is the radius of the base circle. The parametric surface $\boldsymbol{\kappa}$ of the wheelset is defined in a reference position corresponding to the steady rolling, which can be seen in Figure 4:

$$\boldsymbol{\kappa}(\chi,\delta) := \begin{bmatrix} c(\chi)\sin\delta \\ \chi \\ c(\chi)\cos\delta \end{bmatrix}, \tag{15}$$

where $c(\chi)$ is the profile of the wheelset given by

$$c(\chi) := \begin{Bmatrix} -R + h\chi \text{ if } \chi \geq 0 \\ -R - h\chi \text{ if } \chi \leq 0 \end{Bmatrix}. \tag{16}$$

Here $h := \tan\alpha$, $\chi \in (-R/h, R/h)$ and $\delta \in [-\pi, \pi)$.

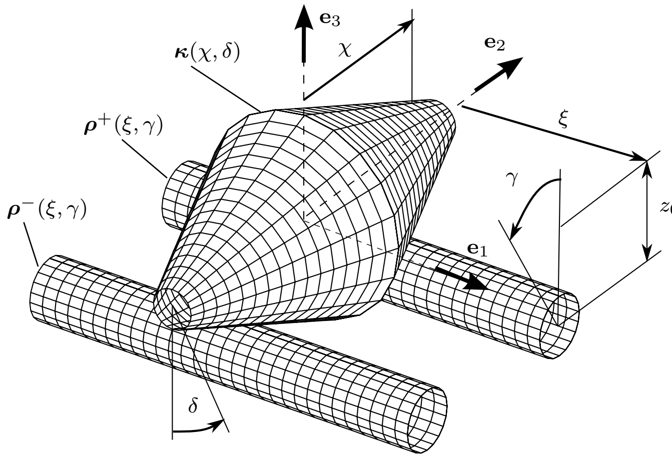

Fig. 4 Surface model of the wheelset and the rails in the reference configuration. The coordinate system is fixed to the rails, but its origin is determined by the geometric centre of the wheelset in the reference configuration. The meshes on the surfaces denote the parameter lines, χ and ξ are measured along the symmetry axes, δ and γ denote angle parameters.

3.4 Contact

A possible method to define a singe-point contact between two surfaces is to keep the surface parameters of the contact point as auxiliary variables, and to prescribe coincidence of the surfaces and their tangent planes at the contact point.

Let us denote the locations of the contact points between the wheelset and the left/right rail by $\xi^{\pm}, \gamma^{\pm}, \chi^{\pm}, \delta^{\pm}$. Then the conditions of coincidence of the contact points are

$$\begin{aligned} \mathbf{u}\big(\boldsymbol{\kappa}(\chi^+,\delta^+)\big) &= \boldsymbol{\rho}^+(\xi^+,\gamma^+), \\ \mathbf{u}\big(\boldsymbol{\kappa}(\chi^-,\delta^-)\big) &= \boldsymbol{\rho}^-(\xi^-,\gamma^-) \end{aligned}, \tag{17}$$

and the equalities of the tangent spaces are

$$\begin{aligned} \mathrm{T}_{(\chi^+,\delta^+)}\mathbf{u}(\boldsymbol{\kappa}) &= \mathrm{T}_{(\xi^+,\gamma^+)}\boldsymbol{\rho}^+, \\ \mathrm{T}_{(\chi^-,\delta^-)}\mathbf{u}(\boldsymbol{\kappa}) &= \mathrm{T}_{(\xi^-,\gamma^-)}\boldsymbol{\rho}^- \end{aligned}, \tag{18}$$

where the symbol $\mathrm{T}_x f$ denotes the tangent space of the function f at a point x. The coincidence and tangent equations are geometric constraints, as they provide algebraic restrictions between the variables.

If pure rolling is assumed at the contact points then the relative velocity between the bodies is zero, that is, the velocities of the wheelset must be zero at the contact points. Mathematically:

$$\begin{aligned} \mathbf{v}\big(\boldsymbol{\kappa}(\chi^+,\delta^+)\big) &= \mathbf{0}, \\ \mathbf{v}\big(\boldsymbol{\kappa}(\chi^-,\delta^-)\big) &= \mathbf{0}. \end{aligned} \tag{19}$$

The rolling constraint is a kinematic constraint, therefore it does not impose a direct restriction on the configuration space, but on the tangent bundle.

3.5 Constant velocity constraint

As we will see later, the prescribed 1D motion of the wheelset along the track determines the evolution of the system through purely kinematic expressions. Therefore we can assume without the loss of generality, that the geometric centre of the wheelset runs at constant velocity v along the track:

$$\mathbf{e}_1 \cdot \mathbf{v}(\mathbf{0}) = v. \tag{20}$$

4 Derivation of the equations of the wheelset

The constraint equations in (17)-(20) are expressed in vector formulation, but they can be reformulated using scalar variables. From the geometric constraints, algebraic equations can be obtained to eliminate some of the variables, the remaining ones are called generalised coordinates. Then the kinematic constraint equations can be transformed to a set of first-order differential equations. This process is straightforward, but the calculations are lengthy. Hence only the main ideas and results are presented.

4.1 Tangency condition

It is expedient to start with the tangency conditions, because some of the variables can be eliminated immediately. The equality of the tangent spaces in (18) is satisfied if the directional derivatives of the surfaces along the parameter lines are all in the same plane. This can be expressed by the equations

$$\Big\langle \partial_1 \boldsymbol{\kappa}(\chi^\pm, \delta^\pm), \partial_2 \boldsymbol{\kappa}(\chi^\pm, \delta^\pm), \partial_1 \boldsymbol{\rho}^\pm(\xi^\pm, \gamma^\pm) \Big\rangle = 0 \tag{21}$$

and

$$\Big\langle \partial_1 \boldsymbol{\kappa}(\chi^\pm, \delta^\pm), \partial_2 \boldsymbol{\kappa}(\chi^\pm, \delta^\pm), \partial_2 \boldsymbol{\rho}^\pm(\xi^\pm, \gamma^\pm) \Big\rangle = 0, \tag{22}$$

where ∂_1 and ∂_2 denotes a partial derivative of a function with respect to its first and second variable, and the angle brackets denote the scalar triple product. Evaluating (21) leads to

$$-c(\chi^\pm)\Big(\sin(\varphi + \delta^\pm)\cos\psi \pm h \sin\psi\Big) = 0. \tag{23}$$

Since $0 < \chi^+ < R/h$ and $-R/h < \chi^- < 0$ then

$$\sin(\varphi + \delta^\pm) = \mp h \tan\psi. \tag{24}$$

From (22) and using (24), we find

$$rc(\chi^\pm)\left(\frac{\pm h}{\cos\psi}\cos(\vartheta + \gamma^\pm) + \sqrt{1 - h^2 \tan^2\psi}\,\sin(\vartheta + \gamma^\pm)\right) = 0, \tag{25}$$

and hence

$$\sin(\vartheta + \gamma^\pm) = \frac{\mp h}{\cos\psi\sqrt{1 + h^2}}. \tag{26}$$

4.2 Coincidence condition

We introduce the following dimensionless parameters:

$$k := \frac{R}{dh} = \frac{R}{d}\cot\alpha, \qquad\qquad l := \frac{rh}{d\sqrt{1+h^2}} = \frac{r}{d}\sin\alpha. \tag{27}$$

It proves effective to work with the difference of the two equations in (17), namely

$$\mathbf{R}\boldsymbol{\kappa}(\chi^+,\delta^+) - \mathbf{R}\boldsymbol{\kappa}(\chi^-,\delta^-) = \boldsymbol{\rho}^+(\xi^+,\gamma^+) - \boldsymbol{\rho}^-(\xi^-,\gamma^-). \tag{28}$$

Then, taking into account equations (24) and (26) the following equations can be obtained:

$$\frac{\chi^+ - \chi^-}{2d} = \frac{(\cos\vartheta\cos\psi - l) - kh^2\sin^2\psi}{\cos^2\psi(1-h^2\tan^2\psi)}, \tag{29}$$

$$\frac{\chi^+ + \chi^-}{2d} = \frac{-\sin\vartheta}{h\sqrt{1-h^2\tan^2\psi}}, \tag{30}$$

$$\frac{\xi^+ - \xi^-}{2d} = -\sin\psi\frac{(\cos\vartheta\cos\psi - l)\,(1+h^2) - kh^2}{\cos^2\psi(1-h^2\tan^2\psi)}. \tag{31}$$

Similarly, if we sum the two equations in (17), we find:

$$\mathbf{R}\boldsymbol{\kappa}(\chi^+,\delta^+) + \mathbf{R}\boldsymbol{\kappa}(\chi^-,\delta^-) + 2\mathbf{x} = \boldsymbol{\rho}^l(\xi^+,\gamma^+) + \boldsymbol{\rho}^r(\xi^-,\gamma^-). \tag{32}$$

After lengthy algebraic manipulation we obtain:

$$\frac{\xi^+ + \xi^-}{2d} = \frac{x}{d} + \frac{\sin\vartheta\sin\psi(1+h^2)}{h\sqrt{1-h^2\tan^2\psi}}, \tag{33}$$

$$\frac{y}{d} = \sin\vartheta\frac{(\cos\vartheta\cos\psi - l)\,(1+h^2) - kh^2}{h\sqrt{1-h^2\tan^2\psi}}, \tag{34}$$

$$\frac{z}{d} = \frac{\cos\psi\sqrt{1-h^2\tan^2\psi}}{h} - \cos\vartheta\frac{(\cos\vartheta\cos\psi - l)\,(1+h^2) - kh^2}{h\sqrt{1-h^2\tan^2\psi}}. \tag{35}$$

Using equations (24), (26), (29)-(31) and (33), we can obtain expressions for all the auxiliary variables $\delta^\pm$,$\gamma^\pm$,$\chi^\pm$ and $\xi^\pm$, while (34) and (35) give geometric constraints for y and z. A configuration space consisting of the generalised coordinates $(\psi,\vartheta,\varphi,x)$ is obtained describing the motion of the wheelset restricted to the single-point contact.

4.3 Velocity conditions

Similarly to the coincidence constraints, the sum and difference of equations (19) are investigated. From the difference we have

$$\boldsymbol{\Omega}\boldsymbol{\kappa}(\chi^+,\delta^+) - \boldsymbol{\Omega}\boldsymbol{\kappa}(\chi^-,\delta^-) = \mathbf{0}. \tag{36}$$

Three linear equations can be obtained for $\dot{\vartheta}, \dot{\psi}$ and $\dot{\varphi}$, but only two of them are independent due to the anti-symmetry of the angular velocity tensor with $\det \boldsymbol{\Omega} = 0$. These scalar equations are

$$\dot{\psi}\frac{\cos\vartheta\cos\psi - l}{\cos^2\psi} + \dot{\varphi}\sin\vartheta = 0, \tag{37}$$

$$\dot{\varphi}h^2\left(k - \frac{\cos\vartheta\cos\psi - l}{\cos^2\psi}\right)\sin\psi - \dot{\vartheta}\frac{\cos\vartheta\cos\psi - l}{\cos^2\psi}(1 - h^2\tan^2\psi) = 0. \tag{38}$$

Similarly, the sum of equations (19);

$$\boldsymbol{\Omega}\left(\boldsymbol{\kappa}(\chi^+,\delta^+) - \mathbf{x}\right) + \boldsymbol{\Omega}\left(\boldsymbol{\kappa}(\chi^-,\delta^-) - \mathbf{x}\right) + 2\dot{\mathbf{x}} = \mathbf{0} \tag{39}$$

leads to three equations. Two of these equations can be derived by using the time derivatives of (34) and (35). That is not surprising, because the coincidence constraint disables the motion of the contact point in a direction normal to the surfaces. Therefore only one new scalar equation arises from (39):

$$-\dot{\varphi}h^2\left(k - \frac{\cos\vartheta\cos\psi - l}{\cos^2\psi}\right) + \dot{\psi}\sin\vartheta(1 - h^2\tan^2\psi) + \dot{x}\frac{h\sqrt{1 - h^2\tan^2\psi}}{d\cos\psi} = 0. \tag{40}$$

Equations (37), (38) and (40) are nonholonomic constraints; they cannot be expressed by the generalised coordinates themselves.

The constant velocity constraint (20) can be rewritten as:

$$\dot{x} = v. \tag{41}$$

It is a holonomic constraint, which for $x_0 := x(0)$, becomes

$$x = x_0 + vt. \tag{42}$$

4.4 Equations of motion of the system

Equations (37), (38), (40) and (41) form a system of equations for the time derivatives of the coordinates, from which $\dot{\psi}$, $\dot{\vartheta}$, $\dot{\varphi}$ and $\dot{x}$ can be determined as a function of the configuration variables ψ and ϑ.

If we introduce the notation

$$B(\psi,\vartheta) := \frac{vh}{d}\frac{\sqrt{1 - h^2\tan^2\psi}/\cos\psi}{\frac{\cos\vartheta\cos\psi - l}{\cos^2\psi}\left(k - \frac{\cos\vartheta\cos\psi - l}{\cos^2\psi}\right)h^2 + \sin^2\vartheta(1 - h^2\tan^2\psi)}, \tag{43}$$

then for (37), (38), (40) and (41) we find

$$\dot{\psi} = -\sin\vartheta \cdot B(\psi,\vartheta), \tag{44}$$

$$\dot{\vartheta} = \frac{h^2 \sin\psi}{1 - h^2 \tan^2\psi}\left(k - \frac{\cos\vartheta\cos\psi - l}{\cos^2\psi}\right) \cdot B(\psi,\vartheta), \tag{45}$$

$$\dot{\varphi} = \frac{\cos\vartheta\cos\psi - l}{\cos^2\psi} \cdot B(\psi,\vartheta), \tag{46}$$

$$\dot{x} = v. \tag{47}$$

It can be seen immediately, that the variables φ and x are cyclic, that is, do not have an effect on the evolution of the system. Therefore the kinematic oscillation is determined in the (ψ,ϑ) phase plane, described by (44) and (45).

The above reduction of the dynamics of the nonholonomic railway wheelset model to a plane can also be followed if the Appell-Gibbs formulation of the equations is considered (see [4], p. 61., or [15] for details and examples, and also [18] for a similar approach). The wheelset has 6 DoF without constraints. The tangency condition (18) linked to the coincidence condition (17) results in 2 scalar stationary (time-independent) geometric constraints (34) and (35) for y and z. Then the velocity conditions lead to one scalar non-stationary (time-dependent) geometric constraint (42) for x and 3 nonholonomic (non-integrable) scalar kinematic constraints (37), (38) and (40).

The 3 geometric constraints reduce the number of DoF by 3, while the 3 kinematic constraints reduce the number of DoF by "one and a half", leading to a system of 3 first-order ordinary differential equations (44)-(46) for the Euler-angles. There are no pseudo-velocities left to be introduced, which means that there are no Appell-Gibbs equations left, with which to express the Newtonian dynamics. In this way we arrive again to the notion of kinematic oscillation.

We could have used an approach based on constrained Lagrangian equations. However, the existing redundancy in the kinematic constraint (36) leads to indeterminacy in the contact forces, and difficulties handling the resulting differential-algebraic equations.

4.5 Phase-plane reduction and simplification

The equations (44)-(45) can be simplified even further if a pseudo-independent dimensionless time τ is introduced by

$$\dot{\tau} := B(\psi,\vartheta). \tag{48}$$

Then, the time derivative of any variable f can be transformed to a derivative with respect to τ by the chain rule:

$$f' := \frac{\mathrm{d}f}{\mathrm{d}\tau} = \dot{f}\frac{\mathrm{d}t}{\mathrm{d}\tau} = \frac{\dot{f}}{B(\psi,\vartheta)}. \tag{49}$$

This transformation is acceptable only on the domain where $B(\psi,\vartheta)$ is neither zero, nor diverging to infinity. One can check, that for the physically relevant values of the variables this condition is fulfilled. Hence, equations (44)-(45) become

$$\psi' = -\sin\vartheta, \tag{50}$$

$$\vartheta' = \frac{h^2 \sin\psi}{1 - h^2 \tan^2\psi}\left(k - \frac{\cos\vartheta\cos\psi - l}{\cos^2\psi}\right). \tag{51}$$

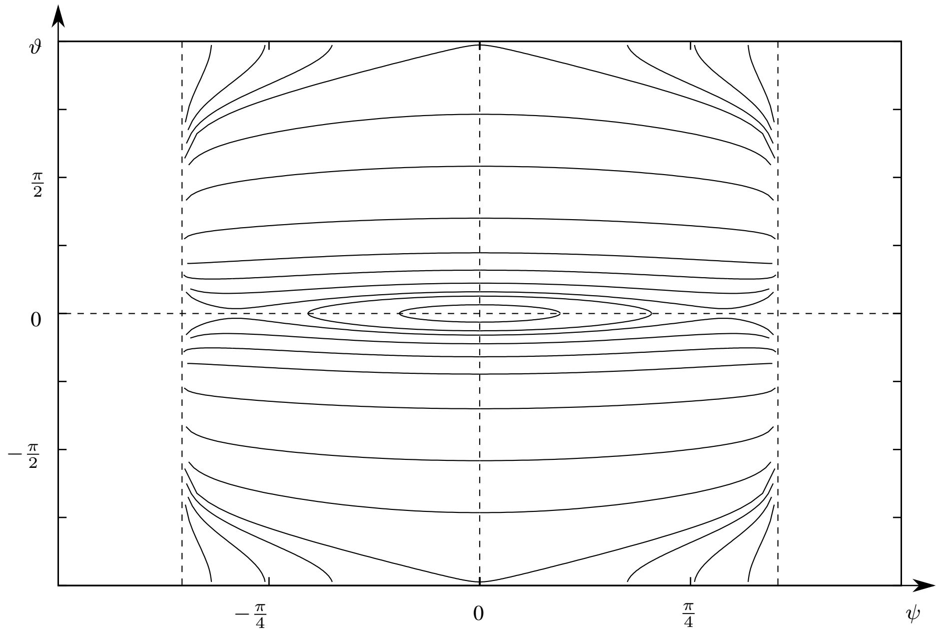

Fig. 5 The phase plane of (50)-(51) for $h = 0.5$, $l = 0.1$, $k = 1.36$, simulated by Runge-Kutta method. The solutions become singular at the vertical dashed lines given by $\tan\psi = \pm 1/h$. Outside these lines the vector field is not defined. The orbit structure is the same if we consider (44)-(45).

This system can be written as a single second order differential equation:

$$\psi'' + \sqrt{1-\psi'^2}\,\frac{h^2 \sin\psi}{1-h^2\tan^2\psi}\left(k - \frac{\sqrt{1-\psi'^2}\cos\psi - l}{\cos^2\psi}\right) = 0. \tag{52}$$

The solution of this equation for $\psi(\tau)$ and $\vartheta(\tau) = -\arcsin\psi'(\tau)$ gives the trajectories for the kinematic oscillation of the wheelset, which can be seen in Figure 5.

5 Stability of steady rolling

Let $X(\psi, \vartheta)$ denote the vector field generated by (44)-(45). We will only consider the physically relevant fixed point of X at the origin, since the two saddles on the ψ axis in Figure 5 are singular points of the original equations (44) and (45). The origin of X corresponds to a steady motion for the full system (44)-(47), given by:

$$\psi \equiv 0, \qquad \vartheta \equiv 0, \qquad \varphi = \varphi_0 + \frac{v}{dh(k-1+l)}t, \qquad x = x_0 + vt. \tag{53}$$

This corresponds to the steady rolling of the wheelset, without kinematic oscillation.

5.1 Stability of the linear system

We now investigate the stability of the origin of X, which corresponds to the stability of the steady rolling to small perturbations in ψ and ϑ. The linearization of X at the origin yields

$$\begin{bmatrix}\dot\psi\\ \dot\vartheta\end{bmatrix} = \begin{bmatrix}0 & a_{01}\\ b_{10} & 0\end{bmatrix}\begin{bmatrix}\psi\\ \vartheta\end{bmatrix} + \mathcal{O}^2(\psi,\vartheta), \tag{54}$$

where

$$a_{01} = \frac{-v}{dh(1-l)(k-1+l)} = \frac{-vd}{R_0 d_0}, \qquad b_{10} = \frac{hv}{d(1-l)} = \frac{hv}{d_0}. \tag{55}$$

The eigenvalues are pure imaginary, hence the linear system has a centre at the origin, and so is neutrally stable. The eigenvalues are denoted by $\pm i\omega$, where

$$\omega := \frac{v}{d(1-l)\sqrt{k-1+l}} = \frac{v}{d_0}\sqrt{\frac{hd}{R_0}} \tag{56}$$

is the natural angular frequency of the small-amplitude kinematic oscillation. Comparing with Klingel's formula (7), we find

$$\frac{\omega_K}{\omega} = \sqrt{1-l} = \sqrt{1-\frac{r}{d}\sin\alpha} \tag{57}$$

Hence Klingel's formula underestimates the accurate value of the natural angular frequency ω. Klingel's formula is valid only for $l \ll 1$ as shown in the right panel of Figure 3. The relative error, approximated by $rh/2d$ for small h, remains around 2-3% in practice, for commonly used geometries of wheelsets and rails see [25], p.2.

5.2 Stability of the weakly nonlinear system

Pure imaginary eigenvalues also correspond to an oscillating solution for the nonlinear centre for small perturbations, but its origin can be either a centre or a spiral point. The Hopf Bifurcation Theorem can be used to characterise such fixed points. The third-order system is given by

$$\begin{bmatrix}\dot\psi\\ \dot\vartheta\end{bmatrix} = \begin{bmatrix}0 & a_{01}\\ b_{10} & 0\end{bmatrix}\begin{bmatrix}\psi\\ \vartheta\end{bmatrix} + \begin{bmatrix}a_{03}\vartheta^3 + a_{21}\vartheta\psi^2\\ b_{30}\psi^3 + b_{12}\psi\vartheta^2\end{bmatrix} + \mathcal{O}^4(\psi,\vartheta). \tag{58}$$

Writing $\tilde\psi = \psi\sqrt{-\omega/a_{01}}$ and $\tilde\vartheta = \vartheta\sqrt{\omega/b_{01}}$, the system can be transformed to

$$\begin{bmatrix}\dot{\tilde\psi}\\ \dot{\tilde\vartheta}\end{bmatrix} = \begin{bmatrix}0 & -\omega\\ \omega & 0\end{bmatrix}\begin{bmatrix}\tilde\psi\\ \tilde\vartheta\end{bmatrix} + \begin{bmatrix}\tilde a_{03}\tilde\vartheta^3 + \tilde a_{21}\tilde\vartheta\tilde\psi^2\\ \tilde b_{30}\tilde\psi^3 + \tilde b_{12}\tilde\psi\tilde\vartheta^2\end{bmatrix} + \mathcal{O}^4(\tilde\psi,\tilde\vartheta). \tag{59}$$

The Poincare-Lyapunov constant λ can be calculated (see for example [27], p.385.) from the second- and third-order coefficients of (59):

$$\begin{aligned}\lambda := {} & \frac{1}{16}(\tilde a_{30} + \tilde a_{12} + \tilde b_{21} + \tilde b_{03}) + \\ & + \frac{1}{16\omega}\left(\tilde a_{11}(\tilde a_{20} + \tilde a_{02}) - \tilde b_{11}(\tilde b_{20} + \tilde b_{02}) - \tilde a_{20}\tilde b_{20} + \tilde a_{02}\tilde b_{02}\right),\end{aligned} \tag{60}$$

where $\tilde a_{ij}$ is the coefficient of the term $\tilde\psi^i\tilde\vartheta^j$. We see here that $\lambda \equiv 0$, because all the coefficients vanish in (60). The Hopf Bifurcation Theorem hence does not help to determine the stability of the system.

5.3 Symmetries and stability of the fully nonlinear system

We can exploit the symmetry properties of our equations to determine the stability of the nonlinear system (44)-(45). The vector field X is called time-reverse symmetric with respect to an invertible mapping G of the phase space onto itself if

$$\mathrm{D}G(\psi,\vartheta)X(\psi,\vartheta) = -X(G(\psi,\vartheta)) \tag{61}$$

for any (ψ,ϑ) in the phase space, where $\mathrm{D}G$ is the gradient tensor of G. The system X, built from (44)-(45), is time-reverse symmetric respect to a reflection in either the $\psi = 0$ or the $\vartheta = 0$ axis:

$$G^1(\psi,\vartheta) := \begin{bmatrix} 1 & 0 \\ 0 & -1 \end{bmatrix} \begin{bmatrix} \psi \\ \vartheta \end{bmatrix}, \qquad G^2(\psi,\vartheta) := \begin{bmatrix} -1 & 0 \\ 0 & 1 \end{bmatrix} \begin{bmatrix} \psi \\ \vartheta \end{bmatrix}. \tag{62}$$

Substituting these into (61), it turns out that these symmetries arise from even and odd properties of the vector field X.

If a system is time-reverse symmetric with respect to a transformation then the trajectories are symmetric. It seems obvious, that the orbits around a spiral point cannot be symmetric with respect to a reflection, but the proof is not trivial. Hence the presence of one of the symmetries G^1 and G^2 is enough to prove that if the origin of the linear system is a centre, then the origin of the nonlinear system is also a centre ([21], p.164.).

In other words, there is a finite neighbourhood around the origin, within which all trajectories are closed. Therefore the steady rolling is neutrally stable.

In general, time-reverse symmetry does not makes the system conservative, but around a centre of a time-reverse symmetric system, a pseudo-energy function can be defined using the closed trajectories as level sets. In this sense the system can be considered conservative in a finite range around the origin.

6 Conclusion

We have investigated the kinematic oscillations of a conical railway wheelset travelling on cylindrical rails with single contact points. For the first time, we derived the exact 3D nonlinear equations, and simplified them to a governing equation in the plane of the yaw and pitch coordinates only (see (52)). From our equations, we have shown the following:

- Klingel's formula for the angular frequency
$$\omega_K = v\sqrt{\frac{h}{R_0 d_0}}$$
of small-amplitude linear oscillations is valid only when
$$\frac{r}{d}\sin\alpha \ll 1$$
(see Figure 3).
- The correct formula for this angular frequency is given by
$$\omega = \frac{\omega_K}{\sqrt{1 - \frac{r}{d}\sin\alpha}}.$$
- For large amplitudes, we have shown that the kinematic oscillations are periodic resulting in neutrally stable steady rolling.

Our results provide an effective numerical challenge for current multibody dynamics software.

Acknowledgements

We thank Professor Istvan Zobory of the Budapest University of Technology and Economics for his advice on the engineering literature. This research was supported by the Hungarian Scientific Research Foundation OTKA under grant no. K101714. The final publication is available at Springer via http://dx.doi.org/10.1007/s11044-014-9424-9.

Erratum

In the final publication, an expression $\sqrt{1-h^2\tan^2\psi}/\cos\psi$ was missing from the formulae (40) and (43).

References

1. Ahmadian, M., Yang, S.: Hopf bifurcation and hunting behaviour in a rail wheelset with flange contact. Nonlinear Dynamics **15**, 15–30 (1998)
2. Ayasse, J.B., Chollet, H.: Wheel-Rail Contact. Book chapter in: S. Iwnicki: Handbook of Railway Vehicle Dynamics. CRC Press (2006)
3. Carter, F.W.: On the action of a locomotive driving wheel. Proc. Royal Society **112**, 151–157 (1926)
4. Gantmacher, F.: Lectures in Analytical Mechanics. MIR Publishers (1975)
5. Gu-ang, Y., de Pater, A.D.: The determination of the nonlinear motion of a railway vehicle. Vehicle System Dynamics **20**, 225–239 (1992)
6. Heumann, H.: Lauf der Drehgestell-Radsatze in der Geraden. Organ für die Fortschritte des Eisenbahnwesens **92**, 149–173 (1937)
7. Hoffmann, M., True, H.: The dynamics of european two-axle railway freight wagons with uic standard suspension. Vehicle System Dynamics **46**, 225–236 (2008)
8. Iwnicki, S.: Simulation of wheel-rail contact forces. Fatigue Fract Engng Mater Struct **26**, 887–900 (2003)
9. Johnson, K.L.: Contact Mechanics. Cambridge University Press (1985)
10. Joly, R.: Etude de la stabilite transversale d'un vehicule ferroviaire. Revue Francaise de Mecanique **36**, 5–26 (1970)
11. Kalker, J.J.: Three-Dimensional Elastic Bodies in Rolling Contact. Kluwer Academic Publishers, Dordrecht (1990)
12. Klingel, J.: Über den Lauf von Eisenbahnwagen auf gerader Bahn. Organ für die Fortschritte des Eisenbahnwesens **38**, 113–123 (1883)
13. Knothe, K.: History of wheel/rail contact mechanics: from Redtenbacher to Kalker. Vehicle System Dynamics **46**, 9–26 (2008)
14. Knudsen, C., Feldberg, R., True, H.: Bifurcations and chaos in a model of a rolling railway wheelset. Phil. Trans. R. Soc. Lond. A **338**, 455–469 (1992)
15. Lewis, A.D.: The geometry of the Gibbs-Appell equations and Gauss's Principle of Least Constraint. Reports on Mathematical Physics **38**, 11–28. (1996)
16. Lorant, G., Stepan, G.: The role of non-linearities in the dynamics of a single railway wheelset. Machine Vibration **5**, 5:18–26 (1996)
17. Murray, R.M., Li, Z., Sastry, S.S.: A Mathematical Introduction to Robotic Manipulation. CRC Press (1994)
18. Ostrowski, J.P., Burdick, J.W., Lewis, A.D., Murray, R.M.: The mechanics of undulatory locomotion: the mixed kinematic and dynamic case. In: Proceedings of the 1995 IEEE International Conference on Robotics and Automation, pp. 1945–1951 (1995)
19. de Pater, A.D.: The equations of motion of a dicone moving on a pair of circular cylinders. Int. J. Non-linear Mechanics **20**, 439–449 (1985)
20. de Pater, A.D.: The geometrical contact between track and wheelset. Vehicle System Dynamics **17**, 127–140 (1988)
21. Strogatz, S.H.: Nonlinear Dynamics and Chaos. Perseus Books (1994)
22. True, H.: On the theory of nonlinear dynamics and its applications in vehicle systems dynamics. Vehicle System Dynamics **31**, 393–421 (1999)

23. Vil'ke, V.: The motion of a railway wheelset. Journal of Applied Mathematics and Mechanics **73**, 385–394 (2009)
24. Wickens, A.H.: The dynamic stability of railway vehicle wheelsets and bogies having profiled wheels. Int. J. Solids Structures **1**, 319–341 (1965)
25. Wickens, A.H.: Fundamentals of Rail Vehicle Dynamics : Guidance and Stability. Swets and Zeitlinger, Lisse (2003)
26. Wickens, A.H.: A History of Railway Vehicle Dynamics. Book chapter in: S. Iwnicki: Handbook of Railway Vehicle Dynamics. CRC Press (2006)
27. Wiggins, S.: Introduction to Applied Nonlinear Dynamical Systems and Chaos, 2nd edn. Springer (2003)
28. Zobory, I.: Prediction of wheel/rail profile wear. Vehicle System Dynamics **28**, 221–259 (1997)